Pressure Measurements and Flow Visualization on a Squeeze Film Damper Operating with a Bubbly Mixture

by

Timothy Beets
Dr. Sergio Diaz
Dr. Luis San Andrés

May 2000

TRC-SFD-2-00

PRESSURE MEASUREMENTS AND FLOW VISUALIZATION IN A SFD OPERATING WITH A BUBBLY MIXTURE

EXECUTIVE SUMMARY

Squeeze film dampers (SFDs) reduce rotor vibrations and control dynamic instabilities in turbomachinery. Depending on damper geometry and operating conditions, the kinematics of journal motion can induce air entrainment and entrapment; produce lubricant vapor cavitation, or both. Air ingestion is the most common condition found in open ended dampers due to the low levels of external pressurization used. The degrading effect of air entrapment on damper performance not only defies predictive models but also constrains the design of SFDs to a costly trial and error process based on prior experience. The present measurements correlate for the first time dynamic squeeze film pressures and pictures of the flow field with the air volume content in the lubricant mixture of a damper performing circular centered motion. The photographs of the flow field at key instances of journal motion show the development of a largely non-homogeneous flow with large gas striated cavities that persist even in the regions of positive dynamic pressures.

ACKNOWLEDGEMENT

The additional support from NSF is gratefully acknowledged.

TABLE OF CONTENTS

LIST OF FIGURES

NOMENCLATURE

C	Damper radial clearance (0.254 mm)
D	Journal diameter (129.4 mm)
e	Orbit radius (0.180 mm)
h	Local film thickness [mm]
L	Damper length (31.1 mm)
Z_0	Axial coordinate of sealed end (0.0 mm)
Z_1	Axial coordinate of first measurement plane (5.6 mm)
Z_2	Axial coordinate of second measurement plane (16.7 mm)
λ	Mixture air volume fraction
ω	Whirl frequency (8.33 Hz)

INTRODUCTION

Controlling rotordynamic instabilities and reducing large amplitude vibrations in turbomachinery are key factors to gain reliability and safety. The squeeze film damper is still widely used to suppress instabilities and dissipate excess vibrational energy in air and land gas turbines. A damper is comprised of a stationary housing, a non-rotating journal attached to the shaft by roller bearings, and a fluid (lubricant) film that occupies the thin clearance between the housing and journal. The fluid film produces a pressure field (and forces) reacting to the dynamic motions of the shaft (journal). The rotor vibratory motion while passing through critical speeds is often an orbital whirl centered within the damper housing [1][1]. The SFD forces reduce the whirling motion and dissipate the excess energy of the rotor bearing system [2, 3].

In operation, the journal dynamic displacements squeeze the film zone immediately ahead in the direction of journal motion, while "stretching" the zone immediately behind the journal [4]. The film pressure in this zone falls below sub ambient conditions and induces air entrainment if exposed to a gaseous surrounding, or lubricant cavitation if the damper operates in a fully submerged condition [5]. As the local film volume increases, the lubricant must show a phase change (vaporization) or release its content of dissolved gases [6]. However, most dampers in practice have their ends open to ambient, and thus air ingestion and entrapment is the prevalent gas introduction mode. Lubricant film rupture leading to vapor cavitation is prominent in dampers operating fully submerged in a lubricant bath or incorporating tight end seals. In an entrained air condition, the entrapped gas readily leads to a (two-phase) bubbly mixture [7, 8]. Quantifiable effects of air entrapment on SFD force performance are of primary importance for their reliable design and practical implementation in high performance turbomachinery.

Diaz and San Andrés [5] conducted experiments on a SFD performing circular centered orbits (CCO) and found a notable reduction in the film peak pressures and damper forces for increasing amounts of air mixed with the pure lubricant. However, using a different test rig and utilizing an impact gun to simulate a transient loading, Diaz and San Andrés [8] performed further tests that revealed larger damping coefficients for air volume fractions (λ) up to 50%. Thus, it appears that air ingestion could lead to contradictory results, i.e. degraded or improved SFD forced performance. However, it has also become obvious that the journal kinematics motion and forced

excitation have a great effect on the bubbly flow field and its ultimate effect on the generated squeeze film pressures and damper reaction forces [9].

Recently, Diaz [10] introduced an analytical model to predict SFD pressures and forces based on the assumption that the lubricant and entrapped air form a homogeneous bubbly mixture. The model predicts the SFD viscous damping coefficient to decrease monotonically with the amount of entrained air for circular centered journal motions. The current investigation focuses on the study of flow patterns within the bubbly film to determine the validity of the homogenous bubbly mixture assumption.

A squeeze film damper test rig revamped to operate with a mixture of lubricant and a controlled volume of air is utilized presently. Dynamic film pressure measurements are conducted for air in oil volume fractions (λ) ranging from 0.0 to 1.0 at a speed of 500 rpm (8.33 Hz whirl frequency). Multiple-period averaging allows the representation of pressure fields that feature the fundamental characteristics of the bubbly flow field [6]. A high-speed photographic camera is also used to identify and record instances of bubbly flow phenomena at various air/oil mixture fractions, and simulating an increasing severity of air entrainment in a typical application. This study is the first to correlate dynamic film pressures and flow patterns of the bubbly mixture with the air volume fraction in the test SFD performing circular centered orbits.

EXPERIMENTAL PROCEDURE

Figure 1 shows a schematic view of the test rig and the nomenclature for designation of the pressure measurement planes (Z_1 and Z_2). The damper journal is supported on ball bearings mounted on an eccentric collar. The collar is press fitted into a nearly rigid shaft that is supported on two ball bearings. Pins allow the journal to perform a whirl orbit, but restrain it from rotating. A DC electric motor drives the shaft through a belt transmission at a desired speed.

The damper housing made of Plexiglas holds several strain-gauge pressure sensors, eddy-current displacement sensors and thermocouples. The journal length *(L)* and diameter *(D)* equal 31.1 mm and 129.4 mm, respectively. The damper radial clearance *(C)* is 0.254 mm (10.0 mils), and the nominal orbit radius (e) is 0.180 mm (7.1 mils). Thus, the dimensionless orbit radius *(e/C)* is 0.71.

---

[1] Numbers in brackets denote cited references listed at the end of the report.

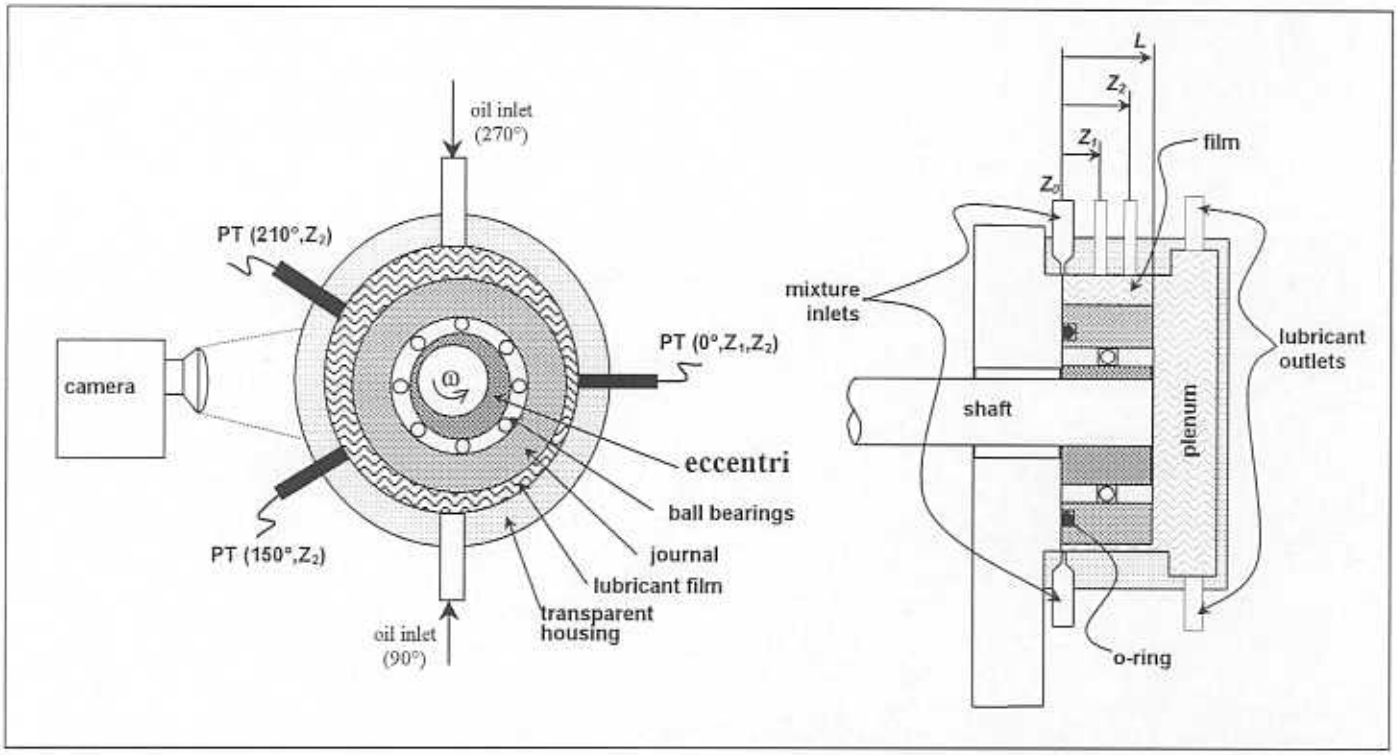

Figure 1. Schematic view of SFD test rig.

A fixed speed gear pump supplies lubricant to the SFD. Pressurized air at 5.44 bar mixes with the lubricant upstream of the SFD inlet through a sparger element. The high supply pressures are needed to avoid the onset of lubricant vaporization at the test whirl frequency of 8.33 Hz (500 rpm). The lubricant is ISO VG 68 oil with density of 0.87 gr/cm^3 and viscosity equal to 77.5 centipoise at 28°C.

The rig instrumentation includes four strain gauge type pressure transducers mounted on two axial planes (one at Z_1 and three at Z_2) and three circumferential positions (two at 0°, one at 150°, and one at 210°; see Figure 1). K-type thermocouples record the lubricant inlet and outlet temperatures. An optical tachometer displays the shaft speed. The journal orbital frequency equals the shaft speed. Two eddy current displacement sensors record the journal motion and provide a direct measurement of the film thickness. All static and dynamic data are recorded in a PC equipped with a virtual instrumentation software package.

A high-speed (1,000 frames per second) digital camera is used to obtain photographs of the air in oil mixture in a window spanning 30° in the circumferential direction and the entire damper axial length. The recorded digital movies allow for real-time play back, slow motion, and frame-by-frame viewing. The pictures properly synchronized with the journal displacements and the

dynamic pressure measurements evidence flow patterns characteristic to the SFD operating condition. Appendix A shows photographs of the test rig and video camera set up while performing flow visualization experiments.

EXPERIMENTAL RESULTS

Figure 2 presents the measured peak-to-peak film pressures for increasing mixture volume fractions at the two axial planes (Z_1, Z_2) of measurement. The tests show that the dynamic film pressures decrease steadily as the air volume fraction (λ) in the lubricant mixture increases. The vertical bars on the graph represent the maximum and minimum temporal fluctuations in the measured pressures due to random variations in the bubbly flow during approximately 16 periods of journal motion. The significant variation of the film pressures for large volumes fraction is displayed, as the bars increase in length for greater air contents in the mixture. The horizontal bars represent the instrumentation uncertainty in estimating the corresponding air in oil volume fraction (λ) at the damper inlet port.

The results in Figure 2 also evidence the reduction in film pressures along the axial length of

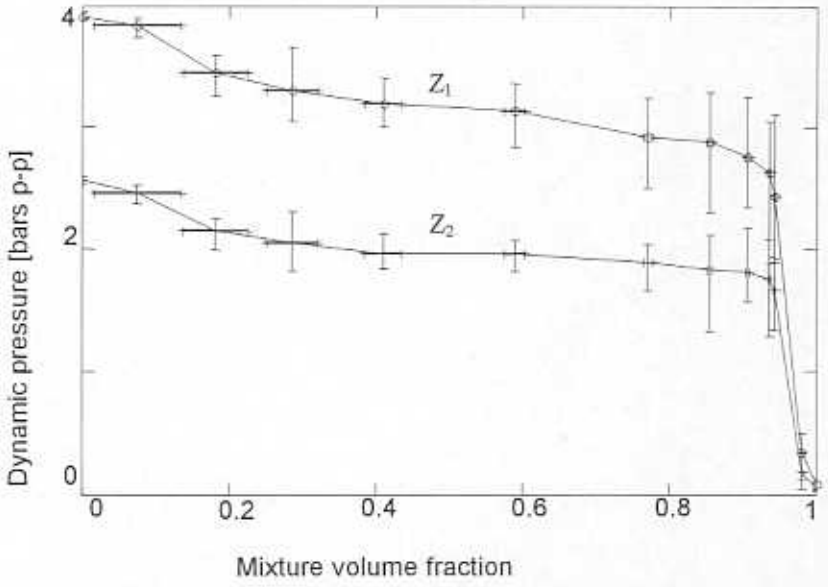

Figure 2. Dynamic peak-peak pressures versus air/oil volume fraction at 0°, Z_1 and Z_2. Whirl frequency 8.33 Hz.

the damper. Higher magnitude dynamic pressures occur at plane Z_1, closer to the sealed end, than at plane Z_2, closer to the damper discharge plane. A period-averaging technique, introduced by Diaz and San Andrés [1], is used to filter the high frequency temporal fluctuations in the measurements of the dynamic pressure fields. Figure 3 represents the period-averaged pressure measurements at *(0°, Z_2)* for a full period of journal motion. This waterfall-type graph shows the reduction in dynamic pressures for increasing air volume fractions. The pressure fields for small air volume fractions denote the characteristics of a pure oil condition. However, as the air content increases, a zone of uniform pressure develops and whose extent grows with an increase in the air volume content in the mixture. The damper is not able to generate measurable hydrodynamic pressures for volume fractions above 0.98. Zeidan and Vance [7] and Diaz and San Andrés [1] forward further arguments explaining the nature of the bubbly mixture pressure distributions.

Figures 4 and 5 illustrate a correlation between the air volume fraction, local film thickness and pressure distributions at *(0°, Z_2)*, and flow pictures captured with the photographic camera. The upper portion of Figure 4 is a contour plot of the pressures depicted in Figure 3. The isobaric lines represent pressure intervals of 0.25 bars, with the minimum and maximum absolute pressures equal to 0.59 and 2.59 bars, respectively. The lower graph in the figure displays the local film thickness corresponding to the dynamic pressures shown in the upper portion of the

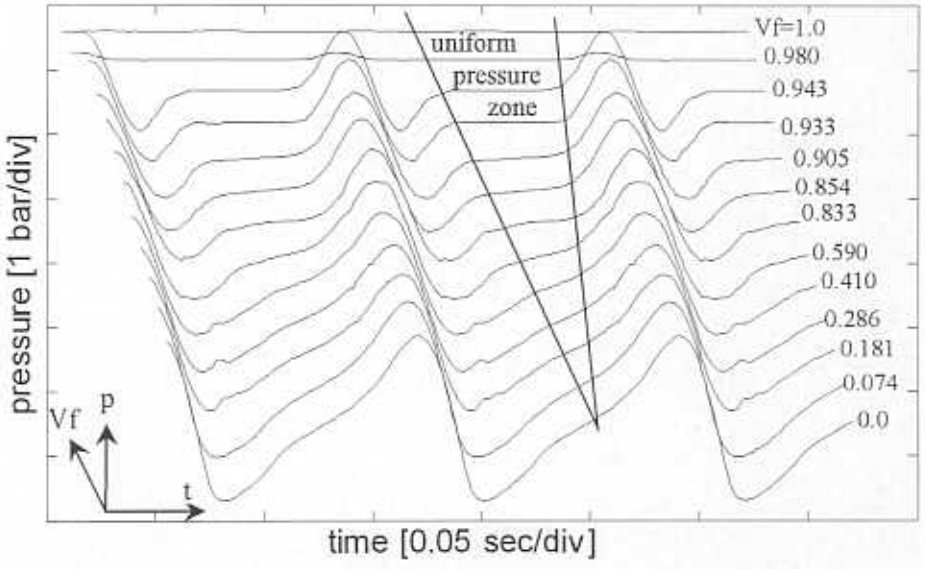

Figure 3. Development of the dynamic pressure field with the air volume fraction at (0°, Z_2). Whirl frequency 8.33 Hz.

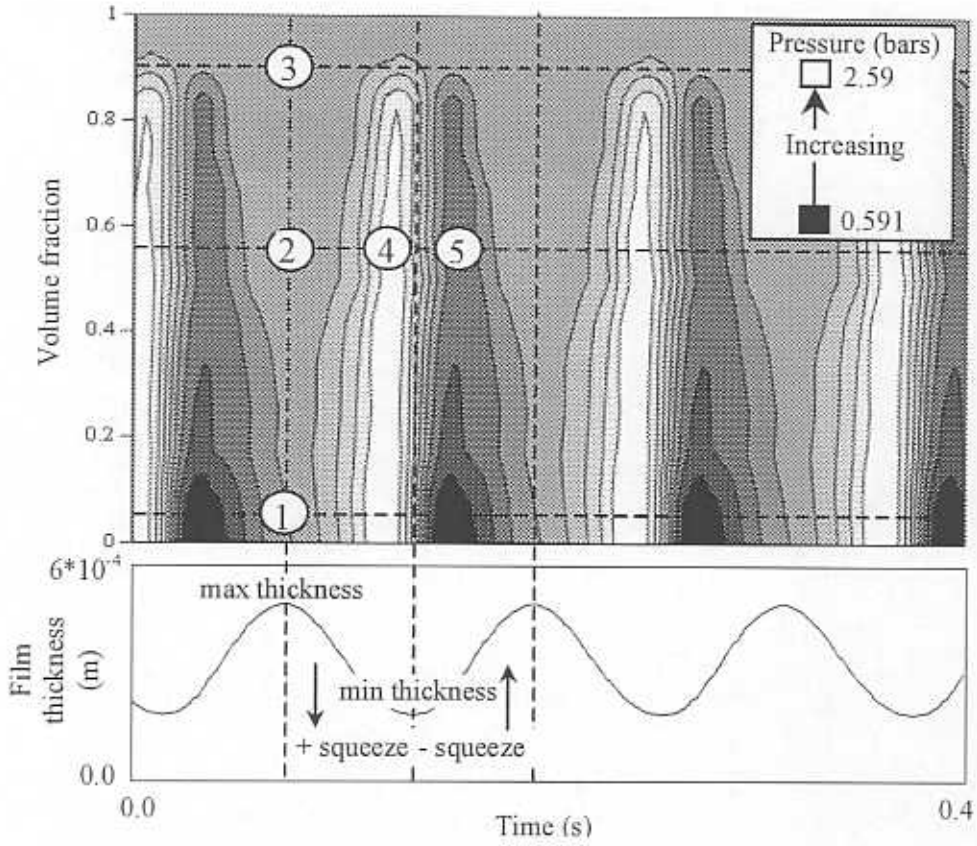

Figure 4. Contour plot of SFD pressure and time related to volume fractions and film Thickness at Location (0°, Z_2).

figure. Figure 5 shows pictures of the squeeze film flow composition at the time and relative journal position shown in Figure 4 for air in oil volume fractions (λ) equal to (1) 0.074, (2) 0.590, and (3) 0.933. These frames correspond to the circled points 1-5 noted in Figure 4.

The local film thickness shows two distinctive events in a period of journal motion. The first one when the journal approaches the housing and decreases the local gap is noted as the positive squeeze action. It is in this half-period when positive (above ambient) film pressures proportional to the time rate of change in film thickness are generated. The negative squeeze action occurs when the local film increases, and which rapidly leads to air entrainment or film rupture in the form of vapor lubricant cavitation.

In the experiments, a sharp drop in pressure follows the region of positive (above ambient) film pressures. After reaching a minimum value, the pressure slightly raises again (still during the

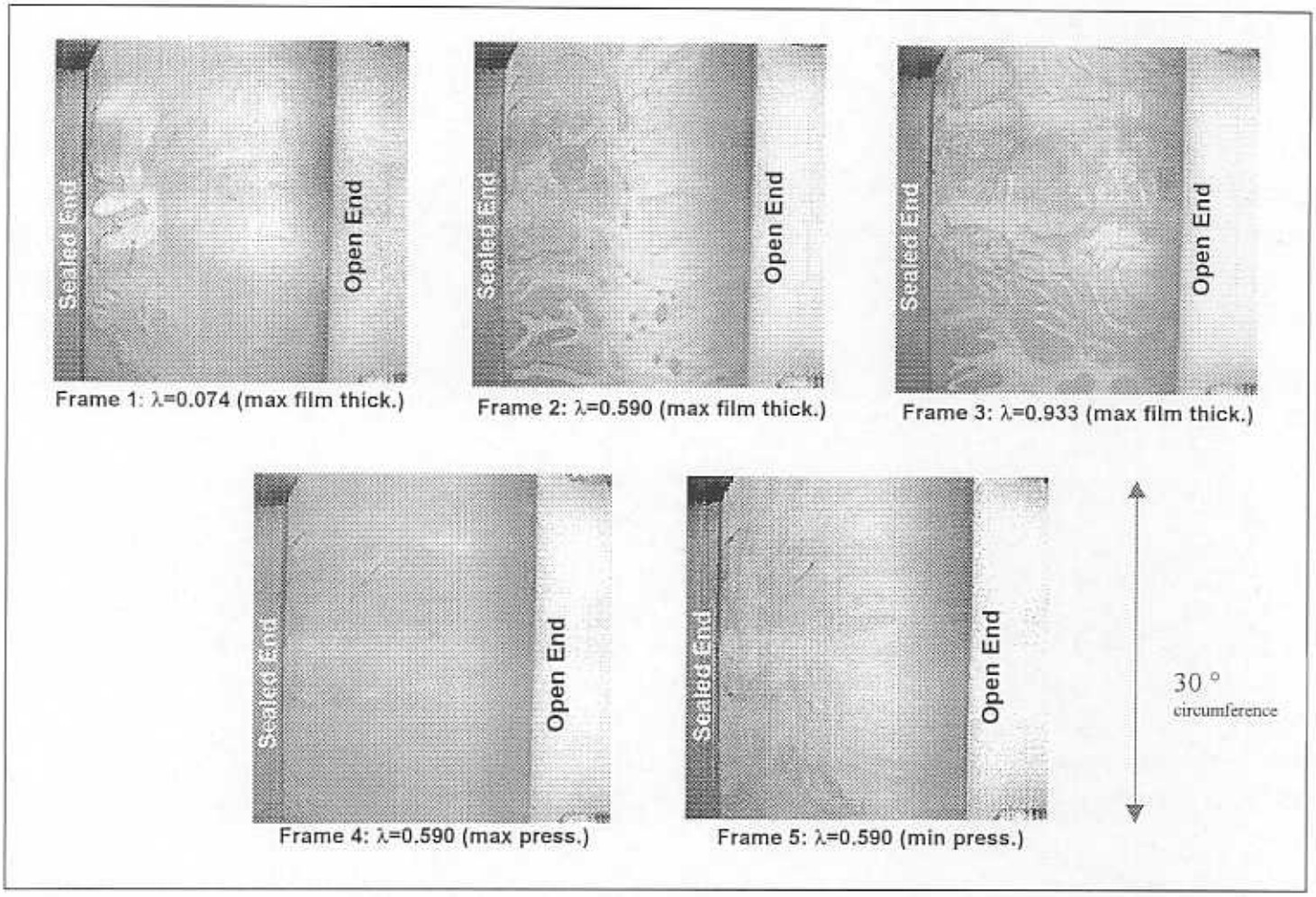

Figure 5. Images of flow recorded by high-speed digital camera. Frames correspond to marked circles on Figure 4.

negative squeeze motion) towards a region of uniform pressure with a magnitude approximately equal to that of the discharge plenum. Note that the plenum is flooded with the lubricant mixture at a pressure of 1.3 bars, slightly higher than ambient. The uniform pressure zone persists for the first fraction of the positive squeeze half cycle; until above ambient pressures develop again as the local film thickness decreases further. Figure 6 depicts this condition for the experiment with a mixture volume fraction equal to 0.59.

Marked Circles 1-3 (see Figure 4) lie in the zone of uniform pressure and coincide with the location of the local maximum film thickness. The fluid mixture contains the greatest amount of gas at this instant where the negative squeeze action of the journal is completed; see Frames 1-3

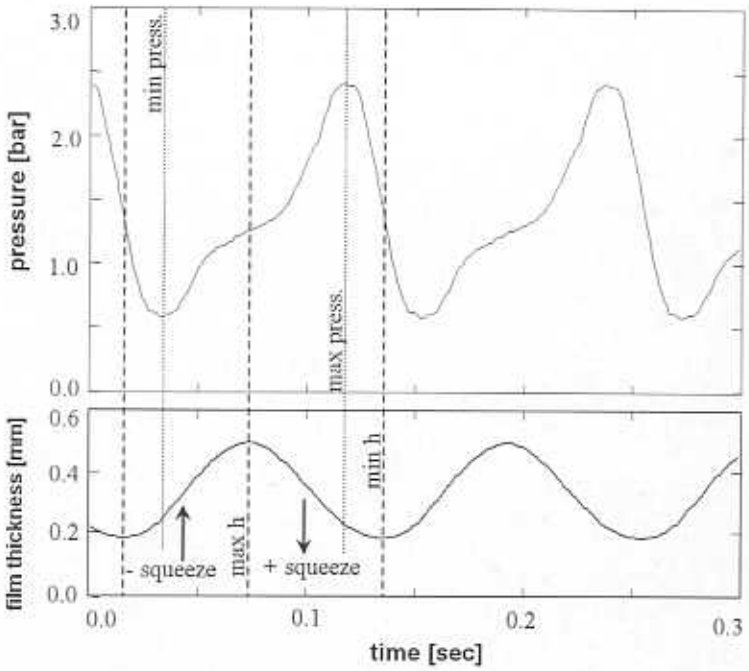

Figure 6. Period averaged pressure field and film thickness at (0°, Z_2) vs. time for volume fraction λ=0.59.

in Figure 5. The mechanical work exerted by the journal brings a large change in the mixture volume at a constant pressure. Frame 1 (Figure 5) shows the image at this instant for a small λ=0.074. The film primarily still consists of a homogenous mixture of very fine air bubbles, whose diameter averages one third of the local film thickness (~0.1 mm), in an oil matrix (foamy oil). However, large bubbles and gas filled striations also exist, surrounded by the mixture close to the sealed end of the damper. Frame 2, for λ=0.590 evidences larger gas striation patterns next to the damper sealed end, with a dense bubble concentration near the center of the journal. The extent of the complex gas cavities ranges from 5 mm to the entire damper length (30.1 mm). Frame 3, for λ=0.933 shows that only a minute amount of pure lubricant remains within the film lands, i.e. oil islands are surrounded by large gas striated cavities.

At the end of the uniform pressure zone, the pressure in the fluid film rapidly increases due to the positive squeeze of the journal (local clearance decreases). As the film thickness decreases to its minimum, the film pressure increases to a maximum. The maximum pressure zone contains a smaller volume of air than any other zone in the pressure cycle. The film at this instant and for a small volume fraction (λ=0.074) consists of a homogenous mixture of lubricant with very fine

bubbles. Frame 4 in Figure 5 displays the flow for λ=0.590, which contains a nearly homogenous mixture with several slightly larger bubbles, dispersed throughout. For increasing volume fractions, and including Frame 3 (λ=0.933), the number and size of the larger bubbles within the mixture increase.

As the local film gap starts to increase, the film pressure decreases from its peak value and falls to a minimum before reaching the uniform pressure zone. These (sub-ambient) pressures pull in air from the foamy mixture at the discharge plenum. Frame 5 displays the image captured at the minimum pressure zone for λ=0.590. The image reveals streaks of air flowing axially from the open end of the journal and converging into a densely packed configuration of growing bubbles near the damper sealed end. As these air bubbles grow with time, fed by the air streaks coming from the discharge, the continuity of the film is interrupted leading to the large gas cavities with striations previously described for the zone of maximum film thickness (Frames 1-3). Note that the same phenomenon is observed for a larger volume fraction, λ=0.933; albeit for this condition, the lubricant film rupture is more intense and with larger and more prevalent gas cavities produced. As the local film thickness keeps increasing, the uniform pressure zone forms, leading again to a condition as that shown in Frames 2 and 3 recorded at the start of a journal cycle. Note that the mixture appeared as a foamy (bubbly) fluid at the discharge plenum in all test conditions.

CONCLUSIONS

Air entrainment and entrapment is a common phenomenon in most practical SFD configurations while undergoing large amplitude journal motions and high whirl frequencies. Hydrodynamic pressures generated by a test SFD performing circular centered motions rapidly decrease with increased amounts of air in the bubbly lubricant mixture. The present study is the first to correlate dynamic film pressures and flow fields with the air volume content and the journal motion.

The photographic study reveals that non-homogenous, large striated cavities of gas, coexist with a "homogeneous" bubbly oil matrix in specific zones determined by the kinematics of the journal motion. For small to moderate air in oil volume fractions, $\lambda < 0.5$, these large cavities are omnipresent, dispersed in the mixture film, but most prominently in a unifrom pressure zone. A few bubbles remain once the dynamic pressure reaches its maximum. However, for greater

volume fractions large air striated cavities remain in the mixture film throughout the entire journal period of motion, and with the greatest concentration and largest sizes in the constant pressure zone. Thus, it appears that the predominant factor in the reduction of the damping force performance in SFDs is the formation and permanence of non-homogenous gaseous cavities within the uniform and high pressure zones of the dynamic squeeze film pressure field.

REFERENCES

[1] Diaz, S. and L. San Andrés, "Reduction of the Dynamic Load Capacity in a Squeeze Film Damper Operating with a Bubbly Lubricant," ASME Paper 98-GT-109, 1998.

[2] San Andrés, L. and J. M. Vance, "Experimental Measurement of the Dynamic Pressure Distributions in a Squeeze-Film Bearing Damper Executing Circular-Centered Orbits," ASLE Transactions, **30**, 3, pp. 373-383, 1986.

[3] Arauz, G. L. and L. San Andrés, "Experimental Pressures and Film Forces in a Squeeze Film Damper." ASME Journal of Tribology, **115**, pp. 134-140, 1993.

[4] Jung, S.Y., L. A. San Andrés, and J.M. Vance, "Measurements of Pressure Distributions and Force Coefficients in a Squeeze Film Damper. Part I: Fully Open Ended Configuration," STLE Tribology Transactions, **34**, 3, pp. 375-382, 1991.

[5] Diaz, S. and L. San Andrés, "Air Entrainment vs. Lubricant Vaporization in Squeeze Film Dampers: An Experimental Assessment of Their Fundamental Differences," ASME Paper 99-GT-187, 1999.

[6] Diaz, S. and L. San Andrés, "Measurements of Pressure in a Squeeze Film Damper with an Air/Oil Bubbly Mixture," STLE Tribology Transactions, **41**, pp.282-288, 1998.

[7] Zeidan, F. and J. M. Vance, "Cavitation Regimes in Squeeze Film Dampers and Their Effect on the Pressure Distribution," STLE Tribology Transactions, **33**, pp. 447-453, 1990.

[8] Diaz, S., and L. San Andrés, "A Method for Identification of Bearing Force Coefficients and its Application to a Squeeze Film Damper with a Bubbly Lubricant," STLE Tribology Transactions, **42**, 4, pp. 739-746, 1999.

[9] Rodriguez, L., Diaz, S., and L. San Andrés, ", Sine Sweep Load Versus Impact Excitations and their Influence on the Identification of Damping in a Bubbly Oil Squeeze Film Damper, " Research Progress Report, TAMU Turbomachinery Research Consortium, May 2000.

[10] Diaz, S. E., "The Effect of Air Entrapment on the Performance of Squeeze Film Dampers: Experiments and Analysis," Ph.D. Dissertation, Texas A&M University, College Station, May 1999.

APPENDIX A

Pictures of SFD test rig and video camera set up while performing measurements